MICROCOPY RESOLUTION TEST CHART

NWC TP 6714

Susceptibility of an Explosive to Premature Reaction in a Penetrating Warhead

by

Marvin E. Backman
for the
Ordnance Systems Department

AUGUST 1986

NAVAL WEAPONS CENTER
CHINA LAKE, CA 93555-6001

DTIC
ELECTE
DEC 2 9 1986

E

REPORT DOCUMENTATION PAGE
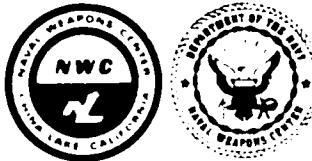
1a. REPORT SECURITY CLASSIFICATION		1b. RESTRICTIVE MARKINGS			
UNCLASSIFIED					
2a. SECURITY CLASSIFICATION AUTHORITY		3. DISTRIBUTION/AVAILABILITY OF REPORT			
2b. DECLASSIFICATION/DOWNGRADING SCHEDULE		Approved for public release; distribution is unlimited.			
4. PERFORMING ORGANIZATION REPORT NUMBER(S)		5. MONITORING ORGANIZATION REPORT NUMBER(S)			
NWC TP 6714					
6a. NAME OF PERFORMING ORGANIZATION	6b. OFFICE SYMBOL (If Applicable)	7a. NAME OF MONITORING ORGANIZATION			
Naval Weapons Center					
6c. ADDRESS (City, State, and ZIP Code)		7b. ADDRESS (City, State, and ZIP Code)			
China Lake, CA 93555-6001					
8a. NAME OF FUNDING/SPONSORING ORGANIZATION	8b. OFFICE SYMBOL (If Applicable)	9. PROCUREMENT INSTRUMENT IDENTIFICATION NUMBER			
Naval Sea Systems Command					
8c. ADDRESS (City, State, and ZIP Code)		10. SOURCE OF FUNDING NUMBERS			
Washington, D.C. 20361		PROGRAM ELEMENT NO 63609N	PROJECT NO 50363-SL	TASK NO	WORK UNIT NO

11. TITLE (Include Security Classification)

SUSCEPTIBILITY OF AN EXPLOSIVE TO PREMATURE REACTION IN A PENETRATING WARHEAD

12. PERSONAL AUTHOR(S)

Backman, Marvin E.

13a. TYPE OF REPORT	13b. TIME COVERED		14. DATE OF REPORT (Year, Month, Day)	15. PAGE COUNT
Final	From 1983	To 1985	1986, August	44

16. SUPPLEMENTARY NOTATION

17. COSATI CODES			18. SUBJECT TERMS (Continue on reverse if necessary and identify by block number)
FIELD	GROUP	SUB-GROUP	Explosive sensitivity, premature reaction, penetrating warhead, shock wave, underwater sensitivity test, penetration impact

19. ABSTRACT (Continue on reverse side if necessary and identify by block number)

(U) This report addresses the problem of correlating explosive reaction in a warhead penetrating a barrier to the stress environment imposed on it. A missile fired against a ship and a missile fired against a concrete structure represent the penetrating impacts of special interest. The emphasis of this work is on the response of the explosive. A standard warhead design was selected because a predictive model was developed from theories of shock generation, transmission and reflection in metals, and existing concepts of initiation of reactions varying from burning to detonation. The model uses equation of state data for the warhead case, barrier and explosive, and wedge test data and underwater sensitivity test data to predict critical combinations of impact speed and barrier

20. DISTRIBUTION/AVAILABILITY OF ABSTRACT		21. ABSTRACT SECURITY CLASSIFICATION		
☐ UNCLASSIFIED/UNLIMITED ☒ SAME AS RPT. ☐ DTIC USERS		Unclassified		
22a. NAME OF RESPONSIBLE INDIVIDUAL		22b. TELEPHONE (Include Area Code)	22c. OFFICE SYMBOL	
Marvin E. Backman		619-939-2206	3894	

DD FORM 1473, 84 MAR

83 APR edition may be used until exhausted
All other editions are obsolete

19. ABSTRACT (Cont'd)

thickness. Sample calculations were performed for three explosive materials. Full-scale tests of warheads on the Supersonic Naval Ordnance Research Track (SNORT) compared to predictions agreed reasonably well.

NWC TP 6714

CONTENTS

ACKNOWLEDGMENT

INTRODUCTION

The defeat of targets that have a protective barrier enclosing vulnerable components requires that, in order to achieve optimum effectiveness, a missile warhead fully penetrate the barrier prior to detonation. The warhead must not only pass through the barrier but also must withstand the dynamic loading imposed on it without losing the functional integrity of essential components. In particular, the explosive charge must survive the dynamic loading without significant reaction. Two examples are of particular interest: (1) A missile fired against a ship target achieves the greatest damage to the ship if the missile perforates the hull and penetrates into the ship's interior without premature initiation of the explosive charge so as to take advantage of the enhancement of damage from confinement. (2) A missile fired against a concrete structure needs to penetrate into the barrier material before detonation in order to achieve confinement and to avoid attenuation of damage by the barrier itself.

This report addresses the problem of correlating explosive reaction to the stress environment imposed on it by a penetrating impact. The process of correlation has two parts The first part looks at interaction between the structural components of the warhead and the barrier. Specifically, the generation of stresses by impact and the subsequent dynamic loading of the explosive. The second part concerns the response of the explosive to dynamic loading. The emphasis of this report will be on the second part. Therefore, the investigation has minimized the variations in warhead configuration in order to achieve maximum clarity in the characterization of explosive response.

To say that a warhead design achieves clarity in the characterization of explosive response to dynamic loading means that in experiments (actual or hypothetical) the design develops all of the relevant and representative aspects necessary for the desired correlation, and the specific details of its configuration and material properties are directly related to the dynamic loading. The section entitled *Background and Approach* discusses the dynamics of impact and explosive sensitivity and shows that structurally robust flat-ended warheads, striking steel plates and concrete slabs at normal incidence, contribute to this kind of clarity.

The section entitled *Predictive Model* describes models for predicting premature reactions in the chosen warhead designs for penetrating impacts against steel plates and concrete slabs. These models integrate the theories and data discussed in *Background and Approach* into a series of comparatively simple analytical procedures by which one can predict the conditions for premature reactions given the impact conditions and warhead and target parameters.

3

BACKGROUND AND APPROACH

DYNAMIC LOADING OF PENETRATOR AND ITS EXPLOSIVE COMPONENTS

The dynamic loading of the explosive components of a penetrating warhead involves a sequence of events that (1) begin with the generation of stresses at the interface between penetrator and barrier (2) followed by the propagation of a distribution of stresses throughout the barrier and the penetrator, and (3) in particular, the application of dynamic loading to the explosive-filled region. Mathematical formulations for the generation of stresses at the interface between projectile and target were part of the earliest work in terminal ballistics (References 1 through 4). In addition, more recent formulations have had at least limited success in predicting the motion of rigid projectiles from specified behavior of deforming media (References 5 through 7). With advances in computer technology, finite element and finite difference formulations of impact problems in terms of continuum mechanical principles have taken advantage of high-speed computers to do the horrendous bookkeeping involved in very fundamental analyses of impact (References 8 through 10). These analyses pose the impact problems as boundary value problems for the partial differential equations that express the basic conservation laws of physics and a constitutive equation that defines material properties. This type of analysis gives solutions for virtually arbitrary configurations and material properties, and the solutions include the details of the development of internal stresses and strains. These predictions of impact phenomena agree with the trends of experimental observations and provide a useful basis for planning and interpreting experiments. Solutions by this method affirm the early dominance of wave propagation in the distribution of stresses and the simplification of phenomena for minimal deformation of the penetrator. Such solutions also substantiate the considerable advantage derived from the use of a flat-ended penetrator.

A flat-ended penetrator striking a plate at normal incidence simultaneously produces a single mechanical state over the entire surface of contact. All other shapes, such as conical or ogival, develop a contact surface at a finite rate of the order of magnitude of the penetration rate. The interactions between the surfaces have varying degrees of development along the surface so that, for example, the stresses from the tip of the pointed penetrator have propagated well into the warhead while the stresses from the most recent contact lie close to the penetrator.

On the other hand, the planar symmetry of the contact surface between the flat-ended penetrator and plate ensures initial states of stress and strain that depend on only one space dimension, and the propagation of this initial state becomes an exercise in one-dimensional wave propagation. The major analytical task becomes that of representing the material responses to the collision of surface. Unfortunately, this initial state of great simplicity soon fades with the propagation of relief effects from the lateral free surfaces. A very crude and simple calculation of the rate of traversal of the barrier and nose plate shows that if the ratio

$$\frac{2h_b + h_n}{D} < 0.5$$

4

where

h_b = the thickness of the barrier
h_n = the thickness of the warhead nose
D = the diameter of the projectile

is applied, then parts of the explosive experience only this simple form of dynamic loading in the early part of the impact.

Clearly, any system, no matter how esoteric, that exhibits such simplifications of behavior has considerable merit as the system of choice in an investigation of the sensitivity of internal explosive components to dynamic loading from impact. It turns out that recent designs of penetrating ordnance have chosen the flat-ended configuration for very practical reasons unrelated to explosive sensitivity, e.g., to achieve yaw stability in the penetration of extended targets (Reference 11). Experimental studies of the stability of penetrators have shown that instability becomes a minimum for the flat-ended nose shape and other investigations show that pointed shapes worsen instability by encouraging cavitational processes that put the center of pressure forward and thus develop an unstable condition. The corner at the edge of the flat-ended penetrator has a strong tendency to increase the efficiency in the penetration of thin plates and it also greatly reduces the tendency to ricochet (References 12 and 13). Thus, the flat-ended nose shape, which promises such significant simplification of the analysis of internal loading, also has direct relevance to existing ordnance. For these reasons, the model described here refers exclusively to a flat-ended cylindrical penetrator with a flat-ended cylindrical explosive-filled cavity. The model's predictions come from the application of plane shock wave theory to the initial stages of the dynamic loading developed in the penetrating impact.

PLANE SHOCK WAVES

For many years, experiments using plane shock propagation have provided most of the information on the behavior of materials at very high pressure and very high strain rate. Explosive plane wave generators (Reference 14) or the impact of cylinders against plate (Reference 15) have developed plane shock waves in materials of interest. Measurements of the propagation rate and particle speeds of these shocks provide the data needed to characterize the materials. The conventional theory of shocks in fluids provides the basis for the interpretation of these experimental measurements. The equations for fluids apply to the solid target and warhead case on the premise that the stresses in the material exceed its yield strength so that the material has lost resistance to shear but not to compression. The behavior of the material then strongly resembles that of a fluid.

The governing equations for one-dimensional shocks come from the application of the principles of the conservation of mass, momentum, and energy to the flow through the shock front. These conservation equations take the form given below (Reference 16).

$$\rho(U - u) = \rho_o U \tag{1}$$

$$P = \rho_o U u \tag{2}$$

$$E - E_o = \frac{1}{2}\left(P + P_o\right)\left(\frac{1}{\rho_o} - \frac{1}{\rho}\right) \tag{3}$$

where

    U = shock speed
    u = particle speed
    P = pressure behind a shock front
    P_o = pressure ahead of a shock front
    E = internal energy behind shock front
    E_o = internal energy ahead of shock front
    ρ = density behind shock front
    ρ_o = density ahead of shock front

Equations 1 and 2 suffice to establish the dependence of the shock speed and the particle speed (u) of the parameters U and ρ. Equation 3, called the Hugoniot equation, expresses the unique properties of specific material. The data needed to determine a particular Hugoniot equation may come from either the equation of state of the material or from measurements of U and u in plane shock experiments. For many materials, the shock and particle speeds have a linear relationship

$$U = a + bu \tag{4}$$

The combination of Equations 2 and 4 determine the dependence of P on u. The equation uses the same information as the Hugoniot equation and comprises an equivalent representation of the behavior of a particular material. The equation in the form

$$P = \rho(a + bu)u \tag{5}$$

has the common name "the direct Hugoniot" to distinguish it from "the reflection Hugoniot," which will be discussed in a later section.

Shock Generation

    Two bodies that collide on plane surfaces with an impact speed, V, abruptly develop a common pressure, P, and a common surface motion, u, over the surface of contact. The pressure and the surface speed belong to wave motions that propagate into each of the colliding bodies. These wave motions serve to accommodate the two bodies to the differences in motion after contact occurs. Due to the abruptness and intensity of the processes, the waves have the form of a shock. The shocks have a common pressure, but each has a particle speed that depends on the Hugoniot, Equation 3, for the particular material

$$P = \rho_1 U_1 u_1 = \rho_2 U_2 u_2 \tag{6}$$

where

$$U_1 = a_1 + b_1 u_1 \tag{7}$$

$$U_2 = a_2 + b_2 u_2 \tag{8}$$

The particle speeds also account for the closure speed so that

$$V = u_1 + u_2 \tag{9}$$

therefore

$$P = \rho_1 U_1 u_1 = \rho_2 U_2 (V - u_1) \tag{10}$$

Figure 1 graphically presents this equation. The two curves represent the direct Hugoniot of material one and the reflection Hugoniot of material two. The latter curve represents the conditions given by

$$P = \rho_2 U_2 (V - u_1) = \rho_2 a_2 (V - u_1) + \rho_2 b_2 (V - u_1)^2 \tag{11}$$

The shock motion in this second body has the opposite direction from that of the first body so that it has a mirror image dependence on the particle speed, U_1, with the intersection of the U axis at $U_1 = V$. Such curves represent the same information as the Hugoniot with the form of Equation 3, but it becomes clear that from equations such as Equation 11, the representation depends on the reference system used for the observation of the particle speed. This kind of situation, in which it becomes convenient to compare particle speed of different directions with respect to a single reference frame, occurs frequently in problems of shock reflection.
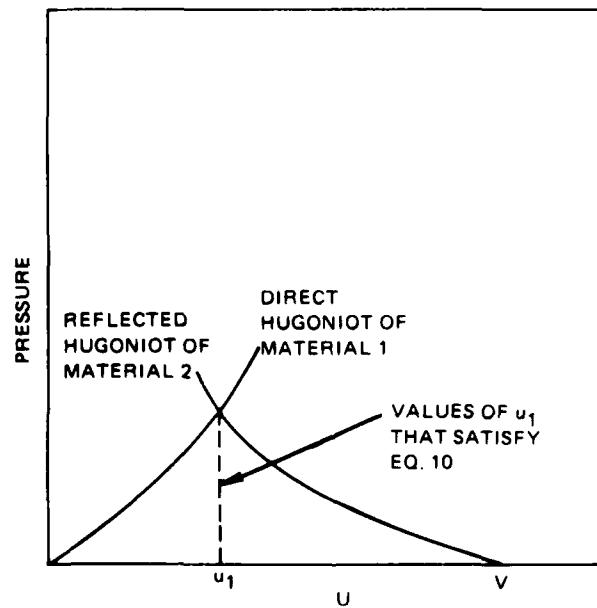

FIGURE 1. Examples of a Direct Hugoniot and a Reflection Hugoniot.

Clearly, if the nose and barrier materials have identical Hugoniot representations (of the form of Equation 3), then the two curves of Figure 1 have a mirror image relationship and the particle speed becomes

$$u_1 = \frac{V}{2} \tag{12}$$

and the pressure

$$P = \rho_1 U_1 \frac{V}{2} = \rho_2 U_2 \frac{V}{2} \tag{13}$$

Shock Attenuation and Wave Shape

At very high stresses, metals behave according to the laws of plasticity rather than the laws of elasticity. Shear components of stress have limitations imposed by the effects of permanent deformation that have the properties of flow and give the material behavior a resemblance to fluid flow. The resemblance to fluid flow increases with the intensity of the applied loads and justifies the use of fluid theory of shocks for impacts greater than a few hundred meters per second. Equations 1 through 3 provide the basis for determining the pressure and particle speed of shock fronts generated by impact according to Equations 5 through 9. These also form the basis for the next section's discussion of the phenomena at interfaces between materials of different properties and interactions among shocks. These predictions all agree with carefully made observations; however, the same kind of careful observations show that other peculiarly solid phenomena enter the process and result in a multiwave system involving more than one propagation rate and the resultant changes of wave shape. Figure 2 shows an experimental measurement of the pressure-time profile made
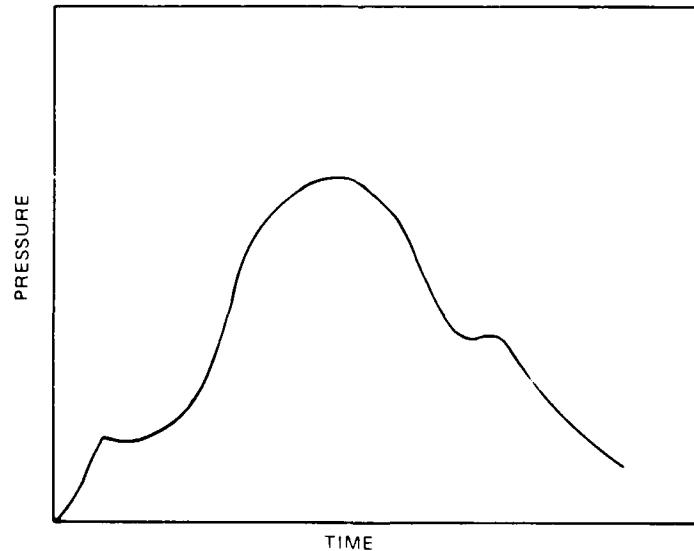

FIGURE 2. Pressure-Time Profile Measured at the Rear Surface of an Explosively-Loaded Mild Steel Plate.

at the rear surface of a plate of mild steel explosively loaded on the front surface (Reference 17). This wave has a typical multiwave structure. The two step-like features propagate at different rates. The wave of lower pressure propagates at the speed of elastic disturbances and has magnitude approximately equal to the dynamic yield value of the material and, thus, corresponds to the residual elastic effects in the plastically deforming body (Reference 18). Phase changes in the solid will also produce additional structure in the forward part of the wave shape (Reference 19). In summary, shock phenomena in metals follow fluid dynamic principles, but the full-wave system exhibits the effects of residual elasticity and phase changes characteristic of the solid material.

The development of the multiwave structure just described and the dissipative processes that occur in a shock result in the attenuation of the wave so that as it propagates, its shape and its amplitude change. The original pressure, P, developed by impact decays to a lower value, $\tilde{P}$. An expression for the attenuation at a distance of propagation, S, based on simple proportionality of the rate of loss of intensity to the instantaneous intensity has the form

$$P_1 = P_o e^{-\alpha S} \tag{14}$$

Experience shows that this simple form adequately describes the net attenuation of many materials. In this simplified description, the one constant, α, covers the net effect of both the development of the multiwave structure and dissipation due to the irreversible processes active in the shock, such as heat conduction and internal viscosity.

Shock Reflection and Transmission

A discontinuity exists in material properties at an interface between two different materials. A shock arriving at such an interface encounters a discontinuity in the Hugoniot that determines the relation between pressure and particle speed. Despite the discontinuous change in material properties, the dynamic state must remain continuous except at a shock front. This can occur by generation of a reflected shock in the material in which the incident shock approached the interface and a transmitted shock in the second material. These shocks establish a new common pressure at the interface and particle speeds in each body consistent with a common motion at the interface.

The Hugoniot for the state of the first material after generation of the reflected shock and in the pressure-particle-speed form (and in the frame of reference for the incident shock) becomes the mirror image of the direct Hugoniot that also passes through the pressure and particle speed of the incident shock (Figure 3). This now represents the state achieved in the first material under the combined incident and reflected waves and with a surface motion of the interface, u_2, (in the original frame of reference). The equation in u_2 for a common pressure at the interface becomes

$$P = \rho_2 U_2 u_2 = \rho_1 U_1 (2u_1 - u_2) = \rho_1 a_1 (2u_1 - u_2) + \rho_1 b_1 (2u_1 - u_2)^2 \tag{15}$$

9
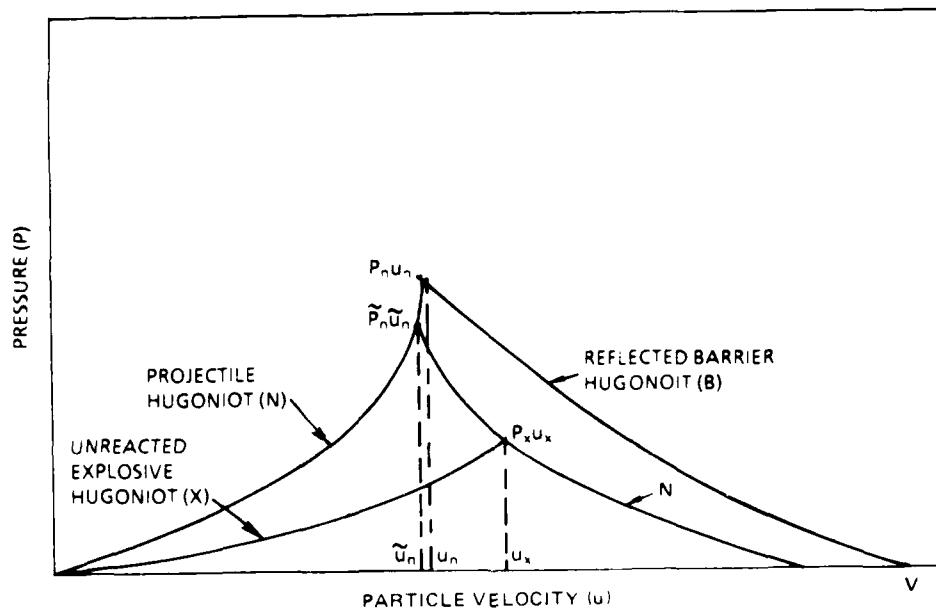
FIGURE 3. Hugoniot Curves Representing the Shock Generation, Reflection, and Transmission for an Impact at Two Plane Surfaces.

where

$$U_1 = a_1 + b_1(2u_1 - u_2)$$

$$U_2 = a_2 + b_2 u_2$$

The expression on the far right side of Equation 15 represents the reflection Hugoniot, i.e., it describes the state of the first material that satisfied the Hugoniot of the first material (in its P - ρ form of Equation 3), but corresponds to surface motions, u_2, under these new conditions of combined incident and reflected shock. Under these new conditions, the particle speed contributed from the reflected shock corresponds to particle speed with the opposite effect on the pressure because reflection has reversed the direction of propagation of the reflected shock. The intersection of this reflected Hugoniot and the direct Hugoniot of the second material established the particular motion of the interface compatible with the discontinuity of material properties.

This kind of process occurs at the interface between the nose plate material and the explosive, and the above principles of "impedance matching" determine the amplitude of the shock that enters the explosive. If the first material has a free surface at which no significant pressure can develop, the Hugoniot for the "second material" collapses to the u-axis, the particle speed becomes twice the incident particle speed, and the pressure after reflection becomes zero. A reflection of this kind cancels the pressure developed at impact and puts a finite duration on the stress wave due to impact.

EXPLOSIVE SENSITIVITY TO SHOCK LOADING

An explosive responds to shock wave loading in a variety of ways. (1) The explosive may detonate almost instantaneously. (2) A low-level chemical reaction may occur and develop into a detonation. (3) A low-level reaction may occur then either dies out or builds in intensity to a destructive level, but not to a true detonation. Many other observations may reflect the importance of some particular characteristic of the warhead, such as the degree of confinement of the region of reaction. The particular response does depend on one or more of the parameters that characterize the shock wave: P, U, u, or T. At high shock pressure greater than a critical pressure, P_d, the shock becomes a detonation wave in times too short to resolve with current measurement techniques.

Above a significant lower threshhold, P_c, the shock and the chemical reaction that it induces develop as distinct but interrelated phenomena. The shock builds up due to the energy fed into it by the chemical reaction, and the chemical reaction builds up due to the greater intensity of the shock. The reaction zone chases the shock as each phenomena augments the other. The process of mutual augmentation continues until it reaches the well-known limit at the conditions for a steady detonation wave This occurs after the shock and reaction zone have traveled a distance that depends on both the initial shock conditions and the explosive, the distance becoming progressively longer for lower shock intensities. Beyond a distance of the order of 20-30 mm, both the shock and the reaction zone die out. If any sustained reaction occurs, it has a different nature. The kind of buildup of reaction just described has the designation shock-to-detonation transfer (SDT) (References 20, 21, and 22).

At still lower pressures, less than a critical pressure (P_c), the shock and chemical reaction become completely distinct phenmena once the shock has initiated the chemical reaction. Experimental studies in this regime, called the low-amplitude long duration shock regime (LALDS), indicate that the impulse in the shock wave correlates to the initiation of sustained burning. Hence, the shock pressure, the pulse duration, and the wave form all enter into the critical conditions for the initiation of burning (Reference 23).

Shock-to-Detonation Transfer

Investigations in the SDT regime have developed a criterion for the transition to detonation that takes the form of a critical energy fluence criterion (Reference 24) given by

$$P^2T = k \qquad (16)$$

where the factor T represents the induction time for the reaction, i.e., the times between the arrival of the pressure and temperatures conditions of the shock front at a given point in the explosive and the manifestation of a significant level of reaction at that same point. Some have defined the level of reaction as the release of 1% of the total available chemical energy.

The minimum pressure for which this kind of reaction occurs corresponds, by Equation 16, to very short times. This virtually guarantees that the duration of the pressure will meet the time requirements for any meaningful barrier thickness. Thus, although the critical criterion for initiation does depend on time, the brevity of the times for all practical purposes makes the initiation dependent only on exceeding a critical pressure, P_c.

Reaction From Large-Amplitude
Long-Duration Shocks

Below the SDT range of pressures is the large-amplitude long-duration shock (LALDS) regime. In the LALDS regime, an equation similar to Equation 16 serves to separate conditions of successful from unsuccessful ignition (Reference 15):

$$P^n T = k \qquad (17)$$

The difference in form has no ready explanation as a phenomenon except that it correspond to broad changes in the physical processes responsible for ignition.

As mentioned above, reactions in the LALDS regime show no sustained coupling between the initiating shock and the reacting region of the explosive. The reaction exhibits accelerated growth but at a far slower rate than for SDT, and the final state of reaction remains separated from the initiating shock and need never have the properties of a detonation. Whereas, SDT appears to result from conditions throughout the region on or near the shock front that favor partial reaction of the explosive material, LALDS involves highly localized responses at very small voids, inclusions, and perhaps other inhomogeneities. A considerable amount of research on the mechanisms of responses to shock in this regime has established the involvement of minute structural or compositional flaws and has provided models for coupling of energy from the shock into the explosive material (Reference 26). For the purposes of this study, one needs a quantification of the submacroscopic processes in terms of macroscopic material properties. For example, the number and size of voids correspond to changes in density. Thus, the sensitivity of an explosive, as measured by the critical pressure (P_c), does in fact increase dramatically with decreases of density from the theoretical maximum density. Other characteristics of the internal structure involve relatively complex measurements that for most materials do not exist. In general, the models for explosive response to shock loading prove inadequate to make predictions in detail, and would require information from expensive tests.

Experiments such as the underwater sensitivity test (Reference 23) establish the dependence of ignition on pressure duration. Apparently the lower pressures cannot produce reactions that have sufficient intensity to propagate forward with a net contribution to the shock strength. However, given an apropriate duration, these pressures can produce reactions of sufficient intensity to result in growth and coalescence of the system of localized reaction into a self-sustaining burn.

CHOICE OF WARHEAD-BARRIER SYSTEM

The susceptibility of explosives to premature reactions during a penetrating impact depends on the dynamic loading applied by the warhead to the explosive and on the particular response of the explosive to this loading. The interaction of the warhead body and the barrier determines the dynamic loading given to the explosive. This study focuses on (1) how an explosive reacts to typical loading and (2) the comparison of various explosives. Therefore, the warhead configuration should remain as constant as possible. Furthermore, the chosen warhead configurations should adequately represent real configurations and allow the most simple and direct correlation of dynamic loading to the warhead and to impact parameters.

The preceding sections have shown the feasibility of such correlations using planar symmetry, e.g., a flat-ended warhead impacting a plate at normal incidence, which represents the conditions encountered by in-service warheads.

The considerations of plane shock phenomena and explosive sensitivity suggest the following limitations on the impact system in order to make the analyses of dynamic loading meaningful and tractable:

1. The warhead has a flat nose configuration that presents a flat surface for contact with the barrier and has a flat-ended explosve-filled chamber with the warhead-explosive interface parallel to the plane of the nose.

2. The warhead has material strength and wall and nose plate dimensions large enough to ensure minimal deformation of the warhead case.

3. The target barrier consists of either a plate of steel or a slab of concrete.

4. A steel barrier has a Hugoniot identical to that of the warhead nose plate.

ASSUMPTIONS AND SIMPLIFICATION

Given the above warhead, the model uses certain assumptions to simplify and expedite the predictive process.

1. The impact pressure pulses have a single wave form with attenuation.

2. The wave shape elongates with attenuation so as to conserve momentum within the pulse.

3. Lateral relief processes determine the wave shape in the thicker concrete targets.

The range of speeds of interest lies between the free-fall speed of the weapon and an upper limit of 2000 ft/s. Most of the data for the validation of predictions lie near 1000 ft/s.

PREDICTIVE MODEL

This section describes a model for characterizing the susceptibility of a given explosive to premature reaction during penetration through either a concrete or a steel barrier. This predictive model presumes the warhead, limitations, assumptions, and simplifications described above. Figure 4 is a flow chart of the predictive model. After the input of data on the barrier, the warhead case, and the explosive, the flow chart has two parallel branches for the steel and concrete barriers. The need for separate treatments arises because the duration of the pressure pulse in the concrete thickness depends only on the lateral relief processes while the steel thickness typically determines the pulse duration.
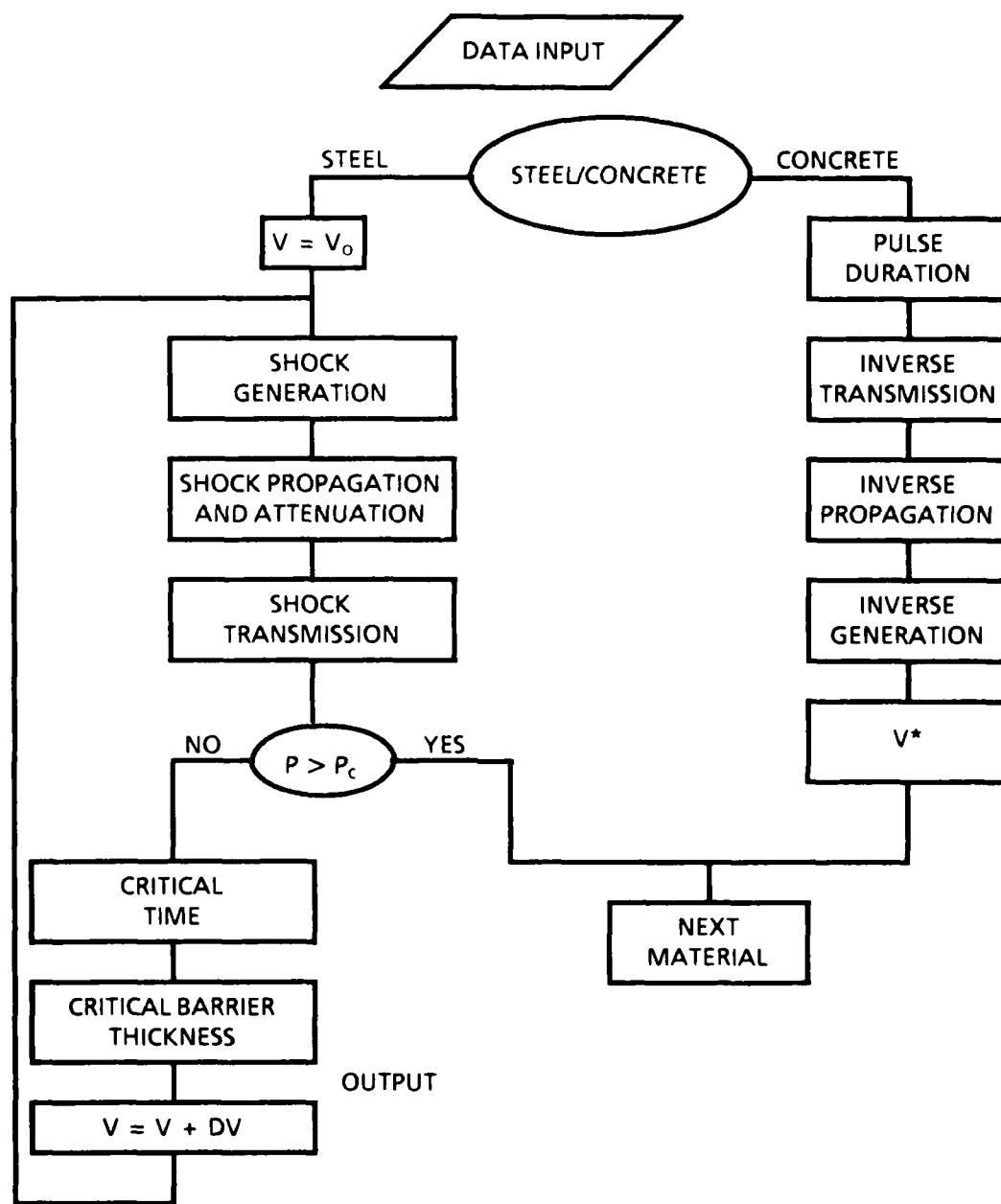
FIGURE 4. Flow Diagram for the Predictive Model.

The steel branch characterizes the explosive by calculating a set of critical impact speeds and the corresponding barrier thicknesses for which the given explosive can exhibit premature reaction. The prediction begins with the calculation of the shock parameters generated by impact at a given impact speed (starting with the minimum speed of interest). The procedure then determines shock attenuation and transmission into the explosive. If the

shock pressure lies below the critical pressure, P_c, for the SDT regime then the shock belongs to the LALDS regime and the calculation of the corresponding critical pulse duration comes from the empirical formulation of the underwater sensitivity tests. The propagation rate for the given impact speed and the thicknesses of barrier determine the barrier thickness that can provide this pulse duration. The process continues with another iteration with a predetermined incremental increase in impact speed until the pressure in the explosive exceeds the value for entry into the SDT regime. At this point, the predictive procedure has completed the correlation of critical impact speed to thickness for the given explosive material.

PREDICTIVE MODEL

PENETRATING WARHEAD DESIGN

This section presents a predictive model for the reaction of an explosive to the dynamic loading from a penetrating impact through either a steel or a concrete barrier. The model incorporates the limitations, assumptions, and simplifications discussed, thus giving an appropriate form for the characterization of the susceptibility of a given explosive to premature reaction as a warhead component. The model assumes a cylindrical steel case surrounding a cylindrical explosive charge. It further assumes strengths and dimensions of the warhead case such that the case avoids any significant deformation during the perforation of the barrier (Reference 27). The barrier consists of either a concrete slab or a steel plate with material behavior identical to that of the warhead nose. The range of delivery speeds does not exceed 2000 ft/s, and the impacts occur at normal incidence. With these stipulations on material behavior, the warhead and barrier meet the criteria of the preceding section for the application of a one-dimensional anaysis of the early phases of the transfer of internal stresses to the explosive fill.

EARLY EVENTS OF IMPACT

Figure 5 shows the nose of a cylindrical warhead with a cylindrical explosive charge at the instant of first contact with the plane face of a concrete slab or a steel plate. The region of this system near the axis of symmetry has planar symmetry so that a simple x-t diagram can represent the motions of its surfaces and the shock fronts that move through it. Consider first the target for which the barrier is a steel plate. Figure 6 shows an example with a thin barrier typical of such a target. The motions have been exaggerated for illustrative purposes. (The figure actually represents a far larger impact speed than this model's limitations would permit.) Below t = 0, the target plate approaches the warhead nose. At t = 0, the contact shown in Figure 5 begins. The surfaces in contact take on a common speed. At the same time, two shocks move out on either side of the surface of contact. These shocks propagate the changes of pressure and particle speed required by the two bodies for compatible conditions at the the surface of contact.
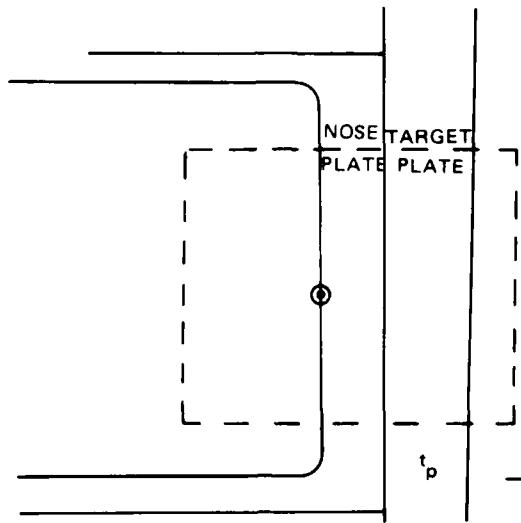
**FIGURE 5.** Drawing of the Contact Region of the Warhead-Barrier Impact System.
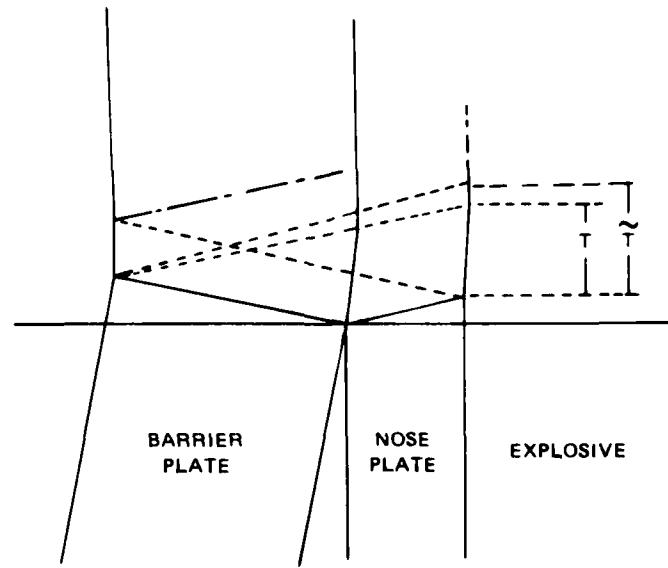
FIGURE 6. An x-t (Lagrange) Diagram of Shock Wave Events of Impact.

The shock front in the nose plate travels to the interface with the explosive where it generates new reflected and transmitted shocks. The transmitted shock begins the dynamic loading of the explosive. Meanwhile, the shock front in the barrier travels to the back where it encounters a free surface from which it generates a reflected wave that reduces the pressure to zero and establishes a particle speed twice that of the incident wave. The reflected wave reaches the contact surface at a time $2h_b/C_b$, where C_b is the propagation speed in the barrier plate which, in general, depends on the particle speed. A new transmitted and reflected shock should occur at this interface, but if the nose plate and the barrier have the same material properties, the shock will pass directy across the interface, bringing the stress-free state into the nose plate. The end of the dynamic loading of the explosive will occur at an interval $2h_b/C_p$ after it began. Under these idealized plane shock loading conditions, the explosive will experience the intensity, P, of the shock transmitted into it for a total duration time, T.

As described already, this phase duration will suffer influences from changes of wave shape and internal processes of attenuation that accompany propagation, but with appropriate corrections, the double transit time provides a prediction of the pulse duration that is needed for the prediction of initiation.

A concrete slab does not have such a simple early phase of loading because it has such a great thickness. In a concrete barrier, lateral relief effects arrive before the reflected wave from the back of the barrier. The time interval, $D/2C_p$, that a relief wave of speed C_p requires to reach the center of the warhead of diameter D provides a rough estimate of the pulse duration. Lateral relief processes lack the simplicity of the longitudinal shock and its reflection.

CHARACTERIZATION OF EXPLOSIVE'S SUSCEPTIBILITY TO PREMATURE REACTION

The described sequence of events applies to all acceptable variations of the system and impact speed. Each of these variations will result in shock parameters P and T that either exceed or do not exceed the critical conditions of Equation 17 and therefore result in either a premature reaction or no reaction. For any given barrier, warhead, and explosive, the model uses Equation 17 to assign a single value of impact speed that separates impacts with premature reactions from those without reactions. The correlation of critical speeds to barrier thickness comprises a measure of the susceptibility of the explosive fill to premature reaction that has its formulation in terms of the conventional parameters for measuring the resistance of the barrier to penetration and the parameter for measuring the penetration potential by the warhead. This characterization applies to a particular nose plate thickness for which it provides the information required to predict the capacity of a particular explosive to survive impact against steel plate barriers. Such a characterization also permits the comparison of different explosives in the same application.

SIMPLE ALGORITHM

The task of predicting the minimum impact speed for premature reaction in a fixed warhead-barrier system requires finding the speed for which the double transit time and the

transmitted pressure simultaneously satisfy Equation 17. The equations are readily written, but it is quickly apparent that these equations do not reduce to an explicit expression for closure speed, V, in terms of the other parameters. The solution requires some kind of iterative process. The closely related task of finding combinations of speed and barrier thickness that satisfy Equation 17 has a far more direct and simple procedure. Given an impact speed, the equations for the generation of impact pressure, its propagation to the metal-explosive interface, and transmission into the explosive (Equations 6 through 15) provide a straightforward means for determning the pressure in the explosive. The equation for the initiation of reaction (Equation 17) determines the critical pulse duration required for initiation; the barrier plate thickness that provides this pulse duration comes from the equation for the double transit time, $T = 2h_b/C_b$.

The following algorithm used this approach to determine a correlation of impact speed to barrier thickness corresponding to the critical conditions for the initiation of reaction in the explosive.

1. Make a systematic choice of impact speed, V.

Example: Choose 1000 ft/s (300 m/s) for the initial speed. If $P_x \leq P_c$ and $T \leq 1$ ms, increase subsequent speed by a predetermined amount, ΔV until $T > 1$ ms.

2. Determine the shock parameters at the contact surface.

$$u_n = V/2 \tag{18}$$

$$P_n = \rho_n \left(a_n + b_n \frac{V}{2} \right) V/2 \tag{19}$$

3. Estimated attenuated values of shock parameters at the metal-explosive interface.

$$\widetilde{P}_n = P_n e^{-\alpha h_n} \tag{20}$$

$$\widetilde{u}_n = \left(-\rho_n a_n + \sqrt{\rho_n^2 a_n^2 + 4\rho_n b_n \widetilde{P}_n} \right) / 2\rho_n b_n \tag{21}$$

4. Calculate shock parameters transmitted across the metal-explosive interface.

$$u_x = \frac{\left(-B + \sqrt{B^2 - 4AC} \right)}{2A} \tag{22}$$

where

$A = \rho_x b_x - \rho_n b_n$

$B = \rho_x a_x + \rho_n a_n + 4\rho_n b_n \widetilde{u}_n$

$C = 2\rho_n a_n \widetilde{u}_n + 4\rho_n b_n \widetilde{u}_n^2$

and

$$P_x = (a_x + b_x u_x)u_x \rho_x \qquad (23)$$

5. Determine the critical pulse duration.

$$T = \frac{k}{P_x^n} \qquad (24)$$

6. Calculate the barrier thickness corresponding to the critical pulse duration.

$$h_b = T\left(\frac{2a_b + b_b V}{4}\right)e^{-ah_n} \qquad (25)$$

Repeat steps 1 through 6 until both the critical pressure for the SDT regime and the pulse duration have been reached. The parameters and the symbols used for them appear in Table 1.

Table 1 lists the 13 parameters that characterize an impact system in this predictive model. At most, 12 of these enter into any given calculation since the barrier and the nose plates have different Hugoniot parameters only in the case of the concrete barrier for which the thickness, h_b, does not enter the calculations. The parameters determine the Hugoniots of the three materials, the thickness parameters of the one-space-dimensional approach, the wave attenuation exponent, and the explosive sensitivity parameters.

TABLE 1. Parameters of the Algorithm for the Penetration of Steel Plates.

Parameter type	Material		
	Barrier	Nose plate	Explosive
Hugoniot	a_b	a_n	$a_.$
	b_b	b_n	$b_.$
	ρ_b	ρ_n	$\rho_.$
Attenuation	...	a	...
Thickness	h_b	h_n	...
Sensitivity	...	...	k
	...	...	n
	...	...	$P_.$

Shock Generation

The generation of plane shocks by the barrier and the nose plate accomplishes the simultaneous and instantaneous accommodation of these bodies to the impact speed, V. In

the general case of different barrier and nose plate materials, the pressure in both waves has a magnitude given by Equation 5

$$P_n = \rho_n(a_n + b_n u_n)u_n \tag{26}$$

$$P_b = \rho_b(a_b + b_n u_b)u_b \tag{27}$$

and for compatible surface speeds

$$u_b = V - u_n \tag{28}$$

so that

$$P_b = P_n = \rho_b \left[a_b + b_b(V - u_n) \right] \left| V - u_n \right| \tag{29}$$

thus

$$(\rho_b b_b - \rho_n b_n)u_n^2 - (2\rho_b b_b V + \rho_n a_n + \rho_b a_b)u_n + (\rho_b a_b + \rho_b b_b V)V = 0 \tag{30}$$

and the solution, which Figure 1 illustrates, has the analytical form

$$u_n = \frac{B + \sqrt{B^2 - 4AC}}{2A} \tag{31}$$

where

$$A = \rho_b b_b - \rho_n b_n$$

$$B = 2\rho_b b_b V + \rho_n a_n + \rho_b a_b$$

$$C = (\rho_b a_b + \rho_b b_b V)V$$

For the special case of steel-on-steel impact, the Hugoniots in Figure 1 become mirror images. Equation 30 reduces by the cancelation of some terms to

$$(2\rho_n b_n V + 2\rho_n a_n)u_n - (\rho_n b_n V + \rho_n a_n)V = 0 \tag{32}$$

which has the solution (Equation 18)

$$u_n = V/2$$

so that Equation 26 becomes Equation 19

$$P_n = \rho_n\left(a_n + b_n \frac{V}{2}\right)V/2$$

Changes of Wave Shape and Attenuation

As the shock generated by impact propagates to the metal-explosive interface, the formation of a multiwave structure and dissipative processes both cause an attenuation of the wave. (The present model makes no attempt to account explictly for an elastic wave or for changes in the shape of the high amplitude wave due to phase changes.) All attenuation effects appear as the exponential decay of Equation 14. Thus, the pressure P_n at the barrier-nose plate interface decays according to

$$\widetilde{P}_n = P_n e^{-ah_n}$$

In order to account for the lengthening of the pulse that accompanies the attenuation, the pulse duration has a compensating elongation

$$\widetilde{T}_n = Te^{-ah_n} \tag{33}$$

so as to conserve the impulse of the wave

$$P_n T = \widetilde{P}_n \widetilde{T} \tag{34}$$

Figure 7 illustrates some of the details of this simplification. It shows the principle features of Figure 6 but with the refinements of an elastic precursor and the representation of the wave reflected from the free surface of the barrier by a set of divergent lines. Each line represents some particular relief pressure value that propagates according to its intensity.
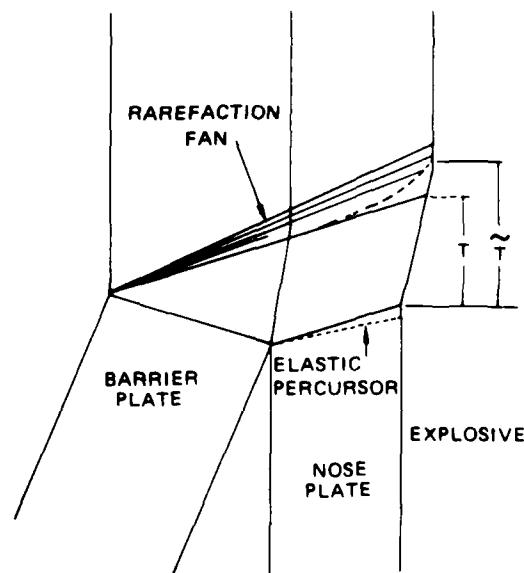
FIGURE 7. An x-t Diagram Illustrating the Simplified Treatment of Attenuation and Change of Wave Shape.

The fan actually has a continuous smear of wavelets. Such a pictorial device more accurately represents the rarefaction process than a single sharp-fronted shock. It implies that the tail of the pressure pulse spreads out in a continuous decline of some sort. The present model replaces these details of rarefaction, the effect of the precursor wave and any other changes of shape with a single decay of a single shock front and a compensating pulse-elongation factor. This simplification accounts for attenuation effects and the known tendency for pulse elongation to accompany attenuation in a simple way and avoids the procedural complexity that a more detailed treatment would necessarily require (and then only by using considerable speculation). The simplification does place a heavy burden on the constant a.

Equation 5 for the attenuated shock becomes

$$\widetilde{P}_n = \rho_n a_n \widetilde{u}_n + \rho_n b_n \widetilde{u}_n^2 \tag{35}$$

The solution of this quadratic equation in $\widetilde{u}_n$ gives the particle speed as a function of the pressure, $\widetilde{P}_n$, and the Hugoniot parameters (Equation 21)

$$\widetilde{u}_n = \frac{-\rho_n a_n + \sqrt{\rho_n^2 a_n^2 + 4\rho_n b_n \widetilde{P}_n}}{2\rho_n b_n}$$

This amounts to finding the new particle speed on the P,u form of the Hugoniot.

Wave Reflection and Transmission

The shock transmitted into the explosive has pressure, P_x, and particle speed, u_x, obtained by the impedance matching process illustrated in Figure 8. The reflected wave proves of no consequence since, as can be seen in Figure 6, it has no effect until well after the cessation of pressure in the explosive by the wave coming from the free surface of the barrier. Continuity of pressure and particle speed require that

$$\rho_x(a_x + b_x u_x)u_x = \rho_n \left| a_n + b_n(2\widetilde{u}_n - u_x) \right| (2\widetilde{u}_n - u_x)$$

which reduces to

$$(\rho_x b_x - \rho_n b_n)u_x^2 + (\rho_x a_x + \rho_n a_n + 4\rho_n b_n \widetilde{u}_n)u_x - (2\rho_n a_n \widetilde{u}_n + 4\rho_n b_n \widetilde{u}_n^2) = 0 \tag{36}$$

and has the solution given by Equation 22

$$u_x = \frac{\left(-B + \sqrt{B^2 + 4AC}\right)}{2A}$$
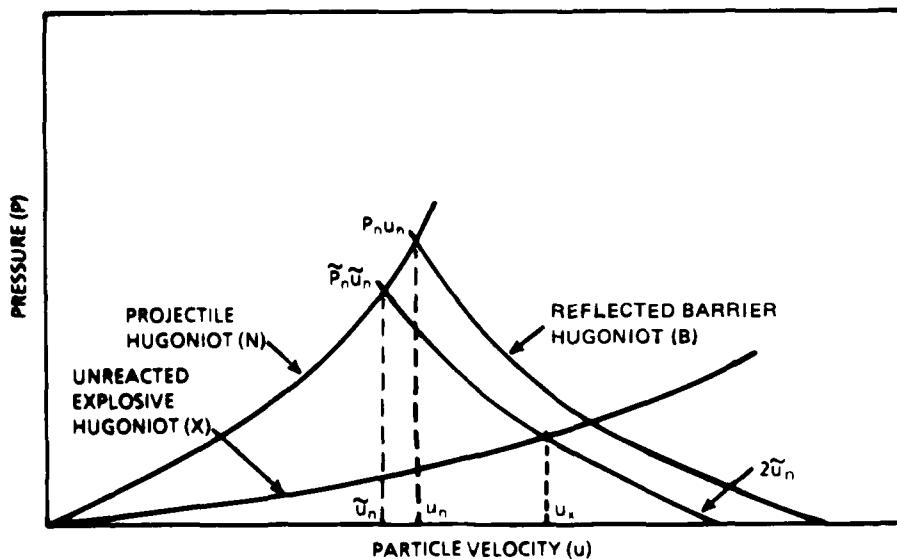
FIGURE 8. Hugoniot Curves for Determining the Particle Speed and Pressure Transmitted into the Explosive Fill.

for

$$A = \rho_x b_x - \rho_n b_n$$

$$B = \rho_x a_x + \rho_n a_n + 4\rho_n b_n \widetilde{u}_n$$

$$C = 2\rho_n a_n \widetilde{u}_n + 4\rho_n b_n \widetilde{u}_n^2$$

so that the pressure in the explosive becomes Equation 23

$$P_x = (a_x + b_x u_x)u_x \rho_x$$

Critical Pulse Duration for Given Pressure

The minimum pulse duration for sustained chemical reaction under the given pressure comes from Equation 17 that summarizes results from underwater sensitivity tests.

$$T = \frac{k}{P_x^n}$$

The model treats this parameter as a sharply defined critical value as a matter of expedience. It gives a deterministic result rather than complicate the procedure with poorly known variance parameters.

23

Critical Thickness Corresponding to
Given Impact Speed

The thickness of the barrier that will result in the pulse duration, T, at a given impact speed comes from the back-calculation of the effects of propagation through the nose plate and barrier. The double transit time, T_{2t}, for the shock from an impact speed, V, has the value

$$T_{2t} = \frac{2h_b}{a_b + b_b \frac{V}{2}}$$

so that

$$h_b = T_{2t} \frac{2a_b + b_b V}{4}$$

The critical pulse duration corresponds to the elongation of this time so that according to Equation 33

$$T = T_{2t} e^{a h_n}$$

Therefore,

$$h_b = T e^{-a h_n} \frac{2a_b + b_b V}{4}$$

ALGORITHM FOR PENETRATION THROUGH
CONCRETE BARRIER

Concrete has less strength and less density than steel so that a concrete barrier must have greater thickness than a steel barrier to offer comparable resistance to penetration. Concrete also has a low propagation rate so that

$$\frac{(2h_b + h_n)}{D} > 0.5$$

and lateral relief processes in the warhead occur much earlier than the arrival of the relief wave from the far side of the concrete barrier. The pulse duration for the initial shock loading depends on the arrival time of the lateral relief. The warhead radius divided by the mean propagation rate gives an approximation for the pulse duration

$$T = \frac{D}{2C_p}$$

where the mean propagation rate has the value of the small amplitude longitudinal wave speed in steel. The following algorithm starts with this estimate of pulse duration and back-calculates the impact speed that will generate the critical pressure corresponding to this pulse duration.

1. Calculate the relief time by means of the elastic small amplitude propagation rate

$$T = \frac{D}{2C_p}$$

2. Calculate the pressure, P_x, for this pulse duration, T, and the corresponding particle speed, u_x

$$P_x = \left(\frac{k}{T} \right)^{1/n}$$

$$u_x = \frac{\left(-\rho_x a_x + \sqrt{\rho_x^2 a_x^2 + 4\rho_x b_x P_x} \right)}{2\rho_x b_x}$$

3. Calculate the pressure, P_n, in the nose plate at the steel-explosive interface and the corresponding particle speed, u_n

$$\widetilde{u}_n = \frac{B - \sqrt{B^2 - 4AC}}{2A}$$

for

$A = -4\rho_n b_n$

$B = 2\rho_n a_n - 4\rho_n b_n u_x$

$C = (\rho_n a_n + \rho_x a_x)u_x + (\rho_x b_x - \rho_n b_n)u_x^2$

$$\widetilde{P}_n = \left(a_n \widetilde{u}_n + b_n \widetilde{u}_n^2 \right) \rho_n$$

4. Calculate the initial shock pressure, P_n, and the corresponding particle speed, u_n

$$P_n = \widetilde{P}_n e^{ah_n}$$

$$u_n = \frac{\left(-\rho_n a_n + \sqrt{\rho_n^2 a_n^2 + 4\rho_n b_n P_n} \right)}{2\rho_n b_n}$$

5. Calculate the impact speed, V, that will generate the pressure, P_n, and particle speed, u_n

$$V = \frac{\left(-B + \sqrt{B^2 - 4AC}\right)}{2A}$$

for

$A = \rho_b b_b$

$B = \rho_b a_b - 2\rho_b b_b u_n$

$C = -(\rho_u a_n + \rho_b a_b)u_n + (\rho_b b_b - \rho_n b_n)u_n^2$

SAMPLE CALCULATIONS FOR THREE EXPLOSIVES

Sample calculations for three explosive fills of a penetrating warhead illustrate the use of the preceding algorithms. These provide examples of the impact data, the final results, and how the data and results are presented. The example illustrates the variation in performance of explosives. These sample calculations also indicate the kind of data that are needed to characterize additional explosives.

The general features of the penetrator design were described in the *Penetrating Warhead Design* section. The warhead and explosive parameters required for the algorithm for steel plates and concrete barriers are listed in Table 1. Specific values of the warhead and plate and barrier parameters that have been used in the sample calculations are listed in Table 2. These specific values come from the selection of mild steel for both the penetrator case and the target plates. The penetrator dimensions are those of the heavy wall penetrator (Reference 28). The Hugoniot parameters for mild steel are given in Reference 29. The concrete data are taken from measurements obtained at NWC and reported in informal reports. The attenuation parameter is given as a range of values, 0.01-0.03, estimated from observed shock attenuations in mild steel (Reference 20).

The values of the explosive parameters used in the sample calculations are listed in Table 3. The Hugoniot properties of the explosives were determined by wedge test data reported in Reference 22 (H-6) and Reference 30 (PBXC-117(E) and PBXW-109(E)). The values of the sensitivity parameters came from underwater sensitivity test data (Reference 23) that have been fitted to the form of Equation 17 and are based on extremely limited data (Reference 31).

TABLE 2. Warhead Case and Barrier Parameters.

Parameter type	Material	
	Steel	Concrete
Hugoniot	ρ = 7.85 g/cm^3	ρ = 2.5
	a = 3.85 km/s	a = 2.27
	b = 1.67	b = 2.52
Attenuation	α = 0.01-0.03 (1/mm)	...
Thickness	h = 38.1 mm	h = 609.6 mm

TABLE 3. Explosive Parameters.

Parameter type	Explosive		
	H-6	PBXW-109(E)	PBXC-117(E)
Hugoniot			
ρ	1.71 g/cm^3	1.66 g/cm^3	1.77 g/cm^3
a	1.9 km/s	1.75 km/s	2.4 km/s
b	1.7	2.78	2.47
Sensitivity			
k	8.0	7.19	6.57
n	1.75	2.46	2.05
P_c	13 GPa	13 GPa	13 GPa

The parameters of Tables 2 and 3 were used in the algorithms for steel plates and concrete slabs as indicated by the flow diagram of Figure 4. The steps of the algorithms were formulated as a program PEMEX for a Hewlett Packard 9845 desktop calculator, which was used to expedite the calculations. A printout of PEMEX is given in the appendix. The result of these computations is a locus of critical conditions of speed and barrier thickness for the initiation of reaction. These are shown in Figures 9 through 11. These loci separate speed and barrier thickness combinations that produce no reaction, those below the locus, from combinations that produce an undesirable reaction, those above the locus. Figures 9 and 10 also contain data from heavywall penetrator tests conducted at NWC (Reference 30).
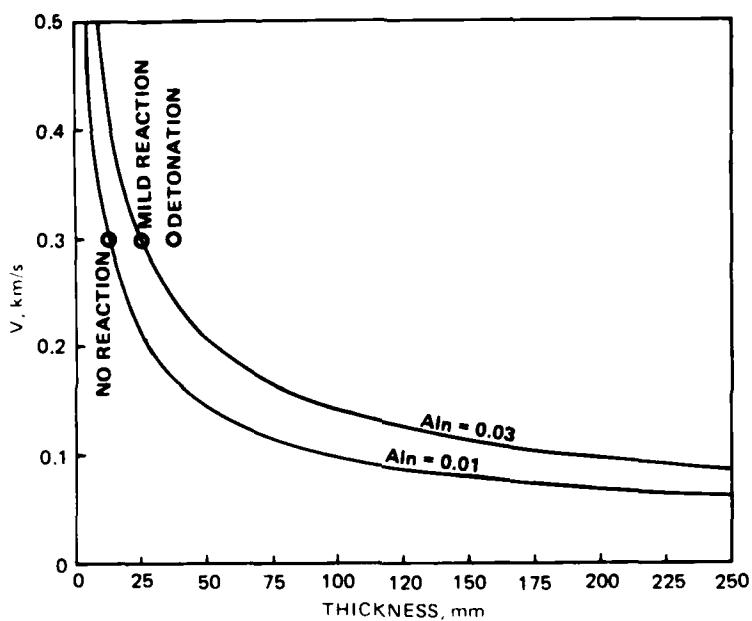
Nose plate:
Rhon = 7.857 g/cm^3
An = 3.85 km/s
Bn = 1.67
Thn = 38.1 mm

Barrier:
Rhob = 7.857 g/cm^3
Ab = 3.85 km/s
Bb = 1.67

Explosive: H-6
Rhox = 1.71 g/cm^3
Ax = 2.83 km/s
Bx = 1.7

Pc = 13 GPa
Ks = 8
Ns = 1.8
Tmax = 1000 μs

FIGURE 9. Critical Speed and Barrier Thickness for the Explosive H-6.
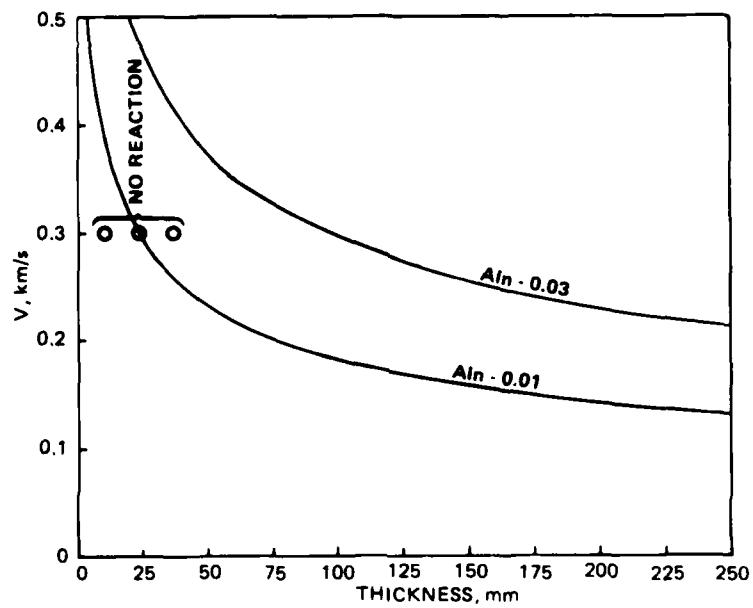
Nose plate:
Rhon = 7.857 g/cm^3
An = 3.85 km/s
Bn = 1.67
Thn = 38.1 mm

Barrier:
Rhob = 7.857 g/cm^3
Ab = 3.85 km/s
Bb = 1.67

Explosive: PBXW-109(E)
Rhox = 1.66 g/cm^3
Ax = 1.75 km/s
Bx = 2.78

Pc = 13 GPa
Ks = 7.2
Ns = 2.5
Tmax = 1000 μs

FIGURE 10. Critical Speed and Barrier Thickness for the Explosive PBXW-109(E).
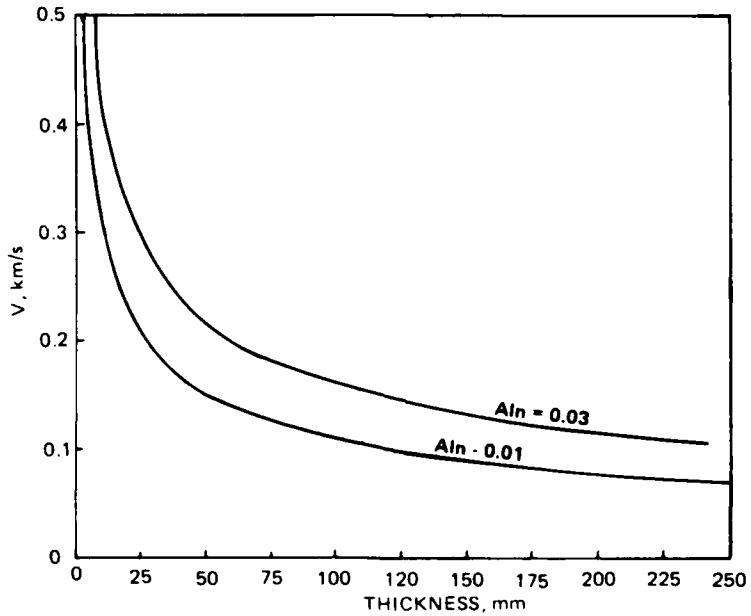
Nose plate:
Rhon = 7.857 g/cm^3
An = 3.85 km/s
Bn = 1.67
Thn = 38.1 mm

Barrier:
Rhob = 7.857 g/cm^3
Ab = 3.85 km/s
Bb = 1.67

Explosive: PBXC-117(E)
Rhox = 1.77 g/cm^3
Ax = 2.4 km/s
Bx = 2.47

Pc = 13 GPa
Ks = 6.6
Ns = 2
Tmax = 1000 µs

FIGURE 11. Critical Speed and Barrier Thickness for the Explosive PBXC-117(E).

CONCLUSIONS AND RECOMMENDATIONS

A model has been developed for predicting premature reactions in the explosive fills of a standard warhead design during perforating impacts. The model requires the equations of state of warhead structural materials and data on the explosive fills derived from underwater sensitivity tests and wedge tests. The model has been applied to steel as the warhead's structural material and three explosives for which the required data are available. A limited amount of full-scale test data has been obtained from sled tests at SNORT. These data show that the model is consistent with this limited amount of data. It is obvious that the model depends strongly on the effective attenuation of shock waves in steel. The attenuation, described by an exponential decay, is actually a complex phenomenon based on the elastic/plastic behavior of steel. From Figures 9 and 10 we can see that a range of values of the attenuation factor are consistent with the model. As more experiments are done, it may be possible to determine the effective attenuation factor more precisely.

The model provides a means for comparing various explosive fills. It also provides a correlation to laboratory tests and, therefore, affords a means for screening explosives for full-scale testing and the data from laboratory testing. Clearly, there is a need for further full-scale testing in which the model can assist in developing a data base on the susceptibility of explosives to premature reaction during penetrating impacts. Through such a testing program the model can be more fully verified and modified.

The model can also be applied to theoretical analysis using finite element or finite differences modes of numerical analyses. Analyses that have already been performed have established the feasibility of this approach. One of the features revealed by the analyses is deformations of the explosive fill that results in separation from the rear surface of the warhead followed by recovery with significant impact speeds on recovery. The model provides a means for assessing the potential for the initiation of violent reactions in this process.

REFERENCES

1. L. Euler. "Neue Grundsatze der Artillerie" (Reprinted from Euler's Opera Omina), Teubaer Berlin (1922).

2. B Robins. "New Principles of Gunnery" (Mathematical Tracts of Late Benjamin Robins, 1), Nourse, London. (1761).

3. E. Opik. *Acta et Communicatus Universitas Jartuensis*, Vol. 28 (1936); also *Irish Astron J.*, Vol. 5, No. 14 (1958).

4. J. D. Murff and H. M. Coyle. *J. Soil Mech.* Foundations Division, Proc. ASCE Vol. 99, No. 1033 (1973).

5. J. V. Poncelet. *Cours De Mechnique Industrielle*, Paris (1829/1835).

6. H. Richter. "Report L.R.S.L. 20/50" (I.S.L.) Franco-German Armament Research Establishment, St. Louis, France, Ballistic Institute (1950).

7. H. Bethe. Report No. UN-41-4-23, Frankfort Arsenal, Ordnance Laboratory (1941).

8. M. L. Wilkins. *Methods in Computational Physics*, Vol. 3. New York, Academic Press (1964), pp. 211-263.

9. T. D. Riney. *High-Velocity Impact Phenomena*. New York, Academic Press (1970), pp. 63-67.

10. R. L. Bjork. *Proceedings of the 10th International Astronomical Congress*, London, 1959.

11. National Defense Research Council. "Effects of Impact and Explosions," NRDC, Div. 2, Vol. 2 (1946), p. 238 (AD 221-586.)

12. R. Recht and T. W. Ipon. "Ballistic Perforation Dynamics," *J. Appl. Mech.*, Vol. 30, Series E, No. 3 (Sep 1963), pp. 384-389.

13. Naval Weapons Center. *Terminal Ballistics*, by M. Backman. China Lake, CA, NWC, February 1976, 90 pp. (NWC TP 5780.)

14. R. G. McQueen et al. "The Equation of State of Solids from Shock Wave Studies," in *High Velocity Impact Phenomena*, ed. by R Kinslow. Academic Press, 1970.

15. Air Force Materials Laboratory. "Experimental Technique and Instrumentation," in *Dynamic Response of Materials to Intense Impulsive Loading*, ed. by P. C. Chou, A. K. Hopkins. 1972.

16. J. Rinehart. "Stress Transients in Solids." Hyper Dynamics, Santa Fe, NM. (1975).

17. C. E. Morris. "Los Alamos Shock Wave Profile Data," University of California Press, Berkeley, Los Angeles, London (1982).

18. NMAB Committee on Materials Response to Ultra-High Loading Rates, "Material Response to Ultra-High Loading Rates," NMAB-356, pp. 58-63. National Materials Advising Board, National Academy of Sciences, Washington, D.C. (1980).

19. G. Duvall. "Applications," in *Dynamic Response of Materials to Intense Impulsive Loading*, ed. by P. C. Chou, A. K. Hopkins, Air Force Materials Laboratory, pp. 485-488. (1972).

20. Naval Ordnance Test Station. *Initiation of Explosives Through Metal Barriers*, by L. N. Cosner and R.G.S. Sewell. China Lake, CA, NOTS, March 1964. (NOTS TP 3489, NAVWEPS Report 8469.)

21. L. Cosner, R.G.S. Sewell, and J. E. Sinclair. "Qualitative Physiochemical Explanation of Initiation and Explosive by Shock Wave," in *Explosivstoffe*, Hdft 10 (October 1969), pp. 230-238.

22. Gibbs and Papolato. "LASL Explosive Property Data," University of California Press, Berkeley, Los Angeles, London (1980), p. 293ff.

23. T. Liddiard. "The Initiation of Burning in High Explosives by Shock Waves," in *Fourth Symposium (International) on Detonation*. Office of Naval Research, Department of the Navy, Washington, D.C. (1965), p. 487ff.

24. F. E. Walker and R. J. Wassle. "Critical Energy for the Shock Initiation of Heterogeneous Explosives," in *Explosivstoffe*, Vol. 17 (1969), pp. 9-13.

25. Naval Weapons Center. "Fragment Initiation of Cased Explosives," in *Airborne Weaponry Technology Program for Surface/Aerospace Weaponry Technology, January-March 1983*. China Lake, CA, NWC, April 1983. (NWC TP 6350-6, Vol. 4.)

26. C. L. Mader. "Numerical Modeling of Detonations," Chapters 3 and 4, University of Califoria Press, Berkeley, Los Angeles, London (1979).

27. Naval Weapons Center. *Finite Element Study of HEP/HED Projectile Penetrating Sand*, by J. C. Schulz and O.E.R. Heimdahl. China Lake, CA, NWC, March 1983. (NWC TP 6417.)

28. Naval Weapons Center. Drawing Package 12934-DLSK 4505438, "Heavy Wall Penetrator Empty Assembly."

29. Stanley P. Marsh. *LASL Shock Hugoniot Data*, University of California Press. (1980).

30. Naval Weapons Center. *PBXW-109E Performance Evaluation* (U), by M. R. Wagenhals and C. D. Lind. China Lake, CA, January 1984. (NWC TM 5103, publication CONFIDENTIAL.)

31. Private communication with R.G.S. Sewell.

Appendix
PREMEX COMPUTER OUTPUT

```
10    ! **************************************************************************
20    !   PREMEX converts Underwater Sensitivity Test Data and Wedge Test Data  !
30    !   into predictions of premature explosive reactions that develop in     !
40    !   penetrating impacts against a variety of barriers by flat-ended       !
50    !   warheads striking at normal incidence.                                !
60    !   **************************************************************************
70    !
80    !   **************************************************************************
90    !                       DIMENSIONED VARIABLES
100   !   **************************************************************************
110       DIM R$[10],Vg(201),Tbg(201),Ed$[12],Nd$[12],Bd$[12],U$[9]
120   !   **************************************************************************
130   !                       OUTPUT OPTIONS
140   !   **************************************************************************
150 Menu: PRINTER IS 16
160       PRINT PAGE
170 *
180       Flag=1
190       Opt=0
200   PRINT "OPTION        FUNCTION"
210   PRINT LIN(1)
220   PRINT "  1           Correlation of Critical Speeds to Critical Barrier"
230   PRINT "              Thicknesses for Thin Metal Barriers"
240       IF Opt=1 THEN Begin
250       PRINT LIN(1)
260   PRINT "  2           A Single Critical Speed for a Thick Slab Barrier"
270       IF Opt=2 THEN Begin
280       PRINT LIN(1)
290   PRINT "  3           A Single Critical Speed for a Thick-metal Barrier"
300   PRINT "              of Given Thickness"
310       IF Opt=3 THEN Begin
320       PRINT LIN(3)
330   INPUT "OPTION",Opt
340       Opt=INT(Opt) MOD 4
350       IF Opt=0 THEN GOTO Menu
360   PRINT PAGE
370       PRINT "OPTION        FUNCTION"
380   ON Opt GOTO 210,250,280
390   !   **************************************************************************
400   !                       BASIC INPUT FOR PROBLEM
410   !   **************************************************************************
420 Begin:    !
430 Nose_plate:  PRINT LIN(2);"Nose-plate characteristics"
440       INPUT "Nose-plate designation (12 characters)",Nd$
450         PRINT "Nose-plate: ";Nd$
460       INPUT "Nose-plate density (gm/cc)",Rhon
470         PRINT "Rhon=";Rhon;" (gm/c)"
480       INPUT "Nose-plate Hugoniot A,B (Km/sec,-)",An,Bn
490         PRINT "An=";An;"(Km/sec) Bn=";Bn
500       INPUT "Nose-plate thickness (mm)",Thn
510         PRINT "Thn=";Thn;" (mm)"
520       IF Opt=2 THEN INPUT "Nose-plate diameter (mm)",Dia
530         IF Opt=2 THEN PRINT "Dia=";Dia;" (mm)"
540         IF (Opt=2) AND (Dia=0) THEN GOTO 520
550       INPUT "Nose-plate attenuation (1/mm)",Aln
560         PRINT "Aln=";Aln;" (1/mm)"
570       IF Opt=2 THEN INPUT "Nose-plate sound speed (Km/sec)",Cp
580         IF Opt=2 THEN PRINT "Cp=";Cp;" (Km/sec)"
590         IF (Opt=2) AND (Cp=0) THEN GOTO 570
600 Barrier: IF Opt<1 THEN GOTO Brrr
610         Rhob=Rhon
620         Ab=An
630         Bb=Bn
640         Bd$=Nd$
650 Brrr:     !
660         R$="Barrier"
```

```
670         IF Opt=2 THEN R$="Slab"
680         PRINT LIN(2);R$;" characteristics"
690         IF Opt>1 THEN DISP "Barrier designation (12 characters)";
700         IF Opt>1 THEN INPUT Bd$
710             PRINT "Barrier: ";Bd$
720         IF Opt>1 THEN INPUT "Barrier density (gm/cc)",Rhob
730             PRINT "Rhob=";Rhob;" (gm/cc)"
740         IF Opt>1 THEN INPUT "Barrier Hugoniots A,B (Km/sec,-)",Ab,Bb
750             PRINT "Ab=";Ab;"(Km/sec) Bb=";Bb
760         IF Opt=3 THEN INPUT "Barrier thickness (mm)",Thb
770             IF Opt=3 THEN PRINT "Thb=";Thb;" (mm)"
780             IF (Opt=3) AND (Thb=0) THEN GOTO 760
790 Explosive:  !
800         PRINT LIN(2);"Explosive characteristics"
810         INPUT "Explosive designation (12 characters)",Ed$
820             PRINT "Explosive: ";Ed$
830         INPUT "Explosive's density (gm/cc)",Rhox
840             PRINT "Rhox=";Rhox;" (gm/cc)"
850         INPUT "Explosive Hugoniot A,B (Km/sec,-)",Ax,Bx
860             PRINT "Ax=";Ax;"(Km/sec) Bx=";Bx;
870             PRINT TAB(40);"[P^Ns*T=Ks, (P in GPA, T in usec)]"
880         INPUT "Critical pressure (GPA)",Pc
890             PRINT "Pc=";Pc;" (GPA)"
900         INPUT "Sensitivity coefficient",Ks
910             PRINT "Ks=";Ks
920         INPUT "Sensitivity exponent",Ns
930             PRINT "Ns=";Ns
940             IF (Opt>1) AND (Ns=0) THEN 920
950     ! ******************************************************************
960     !                   BEGIN THE CALCULATIONS
970     ! ******************************************************************
980         INPUT "Make corrections, then <CONT>",R$
985 Cax=Rhox*Ax
990             Cbx=Rhox*Bx
1000            Can=Rhon*An
1010            Cbn=Rhon*Bn
1020            Cab=Rhob*Ab
1030            Cbb=Rhob*Bb
1040    ! ******************************************************************
1050    !                   OPTION BRANCH POINT
1060    ! ******************************************************************
1070 ON Opt GOTO Opt1,Opt2,Opt3
1080    ! ******************************************************************
1090    !                   OPTION 1
1100    ! ******************************************************************
1110 Opt1:  !
1120        INPUT "Maximum time of interest (usec)",Tmax
1130            IF Tmax<=0 THEN Tmax=1000
1140        Px=Pc
1150        GOSUB Invrse_trnsfr
1160        PRINT LIN(1);"    V=";V;" Km/sec"
1170        INPUT "A better value for V?",V
1180        Delv=V/200
1190        V=V+Delv
1200        MAT Vg=(0)
1210        MAT Tbg=(0)
1220        Mk=1
1230 Opt1_loop:V=V-Delv
1240                IF V<=0 THEN GOTO Draw_graph
1250                Un=V/2
1260            GOSUB Direct_trnsfr
1270                IF Time>Tmax/1E6 THEN GOTO Draw_graph
1280            GOSUB Double_trvsal
1290            Vg(Mk)=V
1300            Tbg(Mk)=Tb
1310                IF Mk=201 THEN GOTO Draw_graph
```

```
1320              Mk=Mk+1
1330              GOTO Opt1_loop
1340  ! ******************************************************************
1350  !                     OPTION 2
1360  ! ******************************************************************
1370 Opt2:   !
1380        Time=Dia/(2*Cp)*1E-6
1390        Px=(Ks/(Time*1E6))^(1/Ns)
1400        GOSUB Invrse_trnsfr
1410             U$="Unrefined"
1420             GOTO Print_data
1430 Opt2_back:    U$="Refined"
1440                 Loops=0
1450 Opt2_loop:    GOSUB Ban_impmat
1460              GOSUB Direct_trnsfr
1470              GOSUB Variab_relief
1480              IF ABS(Dia-Dx)<Dia/1E9 THEN GOTO Print_data
1490              V=V+V*(Dx-Dia)/(Ns*Dia)/2
1500                 Loops=Loops+1
1510              IF Loops<200 THEN GOTO Opt2_loop
1520                 PRINT "V=";V
1530                 IF Loops<250 THEN GOTO Opt2_loop
1540                     PRINTER IS 0
1550                     PRINT LIN(1);"Refined critical speed did not converge
...";LIN(4)
1560                     PRINTER IS 16
1570                     GOTO Menu
1580  ! ******************************************************************
1590  !                     OPTION 3
1600  ! ******************************************************************
1610 Opt3:  !
1620        INPUT "What is your estimate for V?",V
1630                 Loops=0
1640 Opt3_loop:    GOSUB Ban_impmat
1650              GOSUB Direct_trnsfr
1660              GOSUB Double_trvsal
1670              IF ABS(Thb-Tb)<Thb/1E9 THEN GOTO Print_data
1680              V=V+V*(Tb-Thb)/(Ns*Thb)/2
1690                 Loops=Loops+1
1700              IF Loops<200 THEN GOTO Opt3_loop
1710                 PRINT "V=";V
1720                 IF Loops<250 THEN GOTO Opt3_loop
1730                     PRINTER IS 0
1740                     PRINT LIN(1);"Critical speed did not converge...";LI
N(4)
1750                     PRINTER IS 16
1760                     GOTO Menu
1770  ! ******************************************************************
1780  !              INVERSE SHOCK TRANSVERSE
1790  ! ******************************************************************
1800 Invrse_trnsfr:    !
1810        A=Cbx
1820        B=Cax
1830        C=-Px
1840        IF A=0 THEN Ux=-C/B
1850        IF A=0 THEN 1870
1860      Ux=(-B+SQR(B^2-4*A*C))/A/2
1870        A=4*Cbn
1880        B=2*Can-4*Cbn*Ux
1890        C=-((Can+Cax)*Ux+(-Cbn+Cbx)*Ux^2)
1900        IF A=0 THEN Unt=-C/B
1910        IF A=0 THEN 1930
1920      Unt=(-B+SQR(B^2-4*A*C))/A/2
1930      Pnt=Can*Unt+Cbn*Unt^2
1940      Pn=Pnt*EXP(Aln*Thn)
1950        A=Cbn
```

```
1960          B=Can
1970          C=-Pn
1980          IF A=0 THEN Un=-C/B
1990          IF A=0 THEN 2010
2000     Un=(-B+SQR(B^2-4*A*C))/A/2
2010     IF Opt=1 THEN V=2*Un
2020     IF Opt=1 THEN RETURN
2030          A=Cbb
2040          B=Cab-2*Cbb*Un
2050          C=-((Cab+Can)*Un+(Cbn-Cbb)*Un^2)
2060          IF A=0 THEN V=-C/B
2070          IF A=0 THEN 2090
2080     V=(-B+SQR(B^2-4*A*C))/A/2
2090          RETURN
2100  ! *********************************************************************
2110  !                    BARRIER-NOSE IMPEDANCE MATCH
2120  ! *********************************************************************
2130 Ban_impmat:       !
2140          A=Cbb-Cbn
2150          B=-(Cab+Can+2*Cbb*V)
2160          C=Cab*V+Cbb*V^2
2170          IF A=0 THEN Un=-C/B
2180          IF A=0 THEN 2200
2190     Un=(-B-SQR(B^2-4*A*C))/2/A
2200          RETURN
2210          !
2220  ! *********************************************************************
2230  !                    DIRECT-SHOCK TRANSFER
2240  ! *********************************************************************
2250 Direct_trnsfr:    !
2260          Pn=Can*Un+Cbn*Un^2
2270          Pnt=Pn*EXP(-Aln*Thn)
2280             A=Cbn
2290             B=Can
2300             C=-Pnt
2310             IF A=0 THEN Unt=-C/B
2320             IF A=0 THEN 2340
2330       Unt=(-B+SQR(B^2-4*A*C))/A/2
2340             A=Cbn-Cbx
2350             B=-(Can+Cax+4*Cbn*Unt)
2360             C=2*Can*Unt+4*Cbn*Unt^2
2370             IF A=0 THEN Ux=-C/B
2380             IF A=0 THEN 2400
2390       Ux=(-B-SQR(B^2-4*A*C))/A/2
2400          Px=Cax*Ux+Cbx*Ux^2
2410          Time=Ks*Px^Ns/1E6
2420          RETURN
2430  ! *********************************************************************
2440  !                    DOUBLE TRAVERSAL
2450  ! *********************************************************************
2460 Double_trvsal:    !
2470          Tb=Time+((An+Bn*Un)^2)*EXP(-Aln*Thn)*1E5
2480          RETURN
2490  ! *********************************************************************
2500  !                    VARIABLE RELIEF RATE
2510  ! *********************************************************************
2520 Variab_relief:    !
2530          Dx=2*Time*(An+(Bn-1)*Un)*(An+2*Bn*Un)/(An+Bn*Un)*1E6
2540          RETURN
2550  ! *********************************************************************
2560  !                    GRAPHICS OUTPUT
2570  ! *********************************************************************
2580 Draw_graph:    !
2590          IF Keep=1 THEN GOTO Limits_set
2600          PLOTTER IS 13,"GRAPHICS"
2610          Vmax=.00000000001
```

```
2620            IF MAX(Vg(Mk-1),Vg(1))<=Vmax THEN 2650
2630              Vmax=10*Vmax
2640              GOTO 2620
2650              IF Vmax/2<MAX(Vg(Mk-1),Vg(1)) THEN 2680
2660                Vmax=Vmax/2
2670                GOTO 2650
2680            Tbmax=.0000000001
2690            IF MAX(Tbg(Mk-1),Tbg(1))<=Tbmax THEN 2720
2700              Tbmax=10*Tbmax
2710              GOTO 2690
2720              IF Tbmax/2<MAX(Tbg(Mk-1),Tbg(1)) THEN 2750
2730                Tbmax=Tbmax/2
2740                GOTO 2720
2750 Limits_set:   !
2755 Tbmax=250
2760            GRAPHICS
2770            LOCATE 0,120,0,100
2780            SCALE -.2*Tbmax,1.1*Tbmax,-.2*Vmax,1.1*Vmax
2790            LINE TYPE 3
2800            CLIP 0,Tbmax,0,Vmax
2810            IF Keep<>1 THEN GRID Tbmax/10,Vmax/10,0,0
2820            LINE TYPE 1
2830            CLIP -.2*Tbmax,1.1*Tbmax,-.2*Vmax,1.1*Vmax
2840            AXES Tbmax/10,Vmax/10,0,0
2850            MOVE Tbg(1),Vg(1)
2860            FOR L=2 TO Mk-1 STEP 1
2870                DRAW Tbg(L),Vg(L)
2880            NEXT L
2890            MOVE -Tbmax/20,-Vmax/20
2900            CSIZE 3.5
2910            LABEL "0"
2920            MOVE .975*Tbmax,-Vmax/10
2930            LABEL VAL$(Tbmax)
2940            MOVE -Tbmax/10,.99*Vmax
2950            LABEL VAL$(Vmax)
2960            MOVE .9*Tbmax/2,-Vmax/10
2970            LABEL "Th (mm)"
2980            MOVE -Tbmax/10,.9*Vmax/2
2990            LDIR PI/2
3000            LABEL "V (Km/sec)"
3010            LDIR 0
3020            MOVE Tbg(1),1.01*MIN(Vmax,Vg(1))
3030            IF Keep=1 THEN MOVE 1.01*MIN(Tbmax,Tbg(Mk-1)),Vg(Mk-1)/1.02
3040            CSIZE 2.63
3050            LABEL Ed$
3060            DUMP GRAPHICS
3070            EXIT GRAPHICS
3080            GOTO Print_data
3090 ! ***********************************************************
3100 !                   PRINTED OUTPUT
3110 ! ***********************************************************
3120 Print_data:   !
3130        PRINTER IS 0
3140            IF Opt=3 THEN PRINT LIN(1);"Critical speed for thick-metal barrie
r:";V;" (Km/sec)"
3150            IF Opt=2 THEN PRINT LIN(1);U$;" critical speed for thick-slab bar
rier:";V;" (Km/sec)"
3160            IF Opt=1 THEN PRINT "Px=";Px;" (GPA)";TAB(34);"Time= ";Time*1E6;
" (usec)"
3170            PRINT LIN(1)
3180            IF (Opt=2) AND (U$="Refined") THEN GOTO 3330
3190            PRINT "Nose-plate: ";Nd$;TAB(25);"Barrier: ";Bd$;TAB(50);"Explosi
ve: ";Ed$
3200            PRINT LIN(1);
3210            PRINT "Rhon=";Rhon;TAB(25);"Rhob=";Rhob;TAB(50);"Rhox=";Rhox;" (g
/cc)"
```

```
3220            PRINT "An=";An;TAB(25);"Ab=";Ab;TAB(50);"Ax=";Ax;" (Km/sec)"
3230            PRINT "Bn=";Bn;TAB(25);"Bb=";Bb;TAB(50);"Bx=";Bx
3240            PRINT "Thn=";Thn;
3250            IF Opt=3 THEN PRINT TAB(25);"Thb=";Thb;
3260            PRINT " (mm)"
3270            IF Opt=2 THEN PRINT "Dia=";Dia;" (mm)";
3280            PRINT TAB(50);"Pc=";Pc;" (GPA)"
3290            PRINT "Aln=";Aln;" (1/mm)";TAB(50);"Ks=";Ks
3300            IF Opt=2 THEN PRINT "Cp=";Cp;" (Km/sec)";
3310            PRINT TAB(50);"Ns=";Ns
3320            IF Opt=1 THEN PRINT TAB(50);"Tmax=";Tmax;" (usec)"
3330            PRINT LIN(1)
3340            IF (Opt<>2) OR (U$="Refined") THEN PRINT LIN(3)
3350        PRINTER IS 16
3360            IF (Opt=2) AND (U$="Unrefined") THEN Opt2_back
3370            PRINT PAGE
3380 ! *************************************************************
3390 !                    CONTINUE CALCULATIONS
3400 ! *************************************************************
3410            IF Opt=1 THEN Keep=0
3420            IF Opt=1 THEN INPUT "Enter 1 to overlay next curve",Keep
3430            GOTO Menu
3440            END
```

NOMENCLATURE

The symbols used in the text and equations of this report are summarized below in alphabetical order.

A_c, B_c, C_c	Terms in the quadratic formula for the solution of Equations 4 and 9
A_n, B_n, C_n	Terms in the quadratic formula for the solution of Equation 31
A_x, B_x, C_x	Terms in the quadratic formula for the solution of Equation 22
A, B, C	Terms in the quadratic formula for the solution of Equation 45.
a, b	Hugoniot constants
a_1, b_1	Constants for the reflection Hugoniot
a_2, b_2	Constants for the Hugoniot in transmission
a_b, b_b	Constants in the barrier material
a_n, b_n	Constants in the warhead nose
a_x, b_x	Constants in the explosive fill
b_n	Density in a shock in the warhead nose
b_x	Density in a shock in the explosive fill
C	Propagation speed through a material
C_b	Propagation speed through a barrier
C_p	Longitudinal sound speed in steel
D	Diameter of warhead
E	Internal energy behind a shock front
E_0	Internal energy ahead of a shock front
h_b	Thickness of the barrier
h_n	Thickness of the warhead nose
k	Constant in the relation between pressure and pulse duration given by Equation 17
n	Constant in the relation between pressure and pulse duration given by Equation 17
P	Pressure behind a shock front
P_0	Pressure ahead of a shock front
P_x	Pressure in a shock in the explosive
P	Pressure in a shock after attenuation
P_n	Pressure in the nose material of a warhead
P_n	Pressure in the nose material of a warhead after decay of the shock
P_x	Pressure at a shock wave in the explosive
T	Pulse duration
T_{2t}	Pulse duration determined by a relief wave that performs double transit of a given thickness of material

t	Time
U	Shock speed
U_1	Speed of the shock in the material through which an initial shock has been transmitted and reflected from a second
U_1	Particle speed in body 1 during an impact
U_2	Shock speed in a material shocked by transmission from another material
u	Particle speed
u_2	Particle speed in body 2 during an impact
u_b	Particle speed in the barrier during an impact
u_n	Particle speed in the warhead nose during an impact
u_n	Attenuated particle speed in the warhead nose
u_x	Particle speed in the explosive fill
V	Impact speed
V^*	Initial speed for premature reaction
ΔV	Increment of impact speed
a	Attenuation constant
ρ	Density behind a shock wave
ρ_0	Density ahead of a shock wave
ρ_1	Density in the shock developed in body 1 during impact
ρ_2	Density in the shock developed in body 2 during impact
ρ_b	Density in a shock in the barrier

INITIAL DISTRIBUTION

8 Naval Air Systems Command
    AIR-301 (2)
    AIR-320, B. Warren (1)
    AIR-320D (1)
    AIR-5405 (2)
    AIR-723 (2)
5 Chief of Naval Operations
    OP-03 (2)
    OP-05 (1)
    OP-098 (1)
    OP-55 (1)
4 Chief of Naval Research, Arlington
    OCNR-213 (1)
    OCNR-432P, R. Miller (1)
    OCNR-461 (1)
    OCNR-474 (1)
1 Director of Navy Laboratories (DNL-05)
6 Naval Sea Systems Command
    SEA-06G23 (1)
    SEA-06G42 (2)
    SEA-09B12 (2)
    SEA-62R (1)
1 Commander in Chief, U.S. Pacific Fleet (Code 325)
1 Commander, Third Fleet, Pearl Harbor
1 Commander, Seventh Fleet, San Francisco
1 David W. Taylor Naval Ship Research and Development Center, Bethesda
2 Naval Academy, Annapolis (Director of Research)
1 Naval Air Force, Atlantic Fleet
2 Naval Air Force, Pacific Fleet
1 Naval Air Station, North Island
1 Naval Air Development Center, Warminster (Code 813)
2 Naval Air Test Center, Patuxent River (Central Library, Bldg. 407)
1 Naval Avionics Center, Indianapolis (Technical Library)
1 Naval Civil Engineering Laboratory, Port Hueneme (Code L31)
1 Naval Coastal Systems Center, Panama City (Technical Library)
1 Naval Explosive Ordnance Disposal Technology Center, Indian Head
1 Naval Ocean Systems Center, San Diego (Code 447)
4 Naval Ordnance Station, Indian Head
    Code 5246, Technical Library (1)
    Code 5261A, P. Dendor (1)
    PM2C J. Torres (1)
1 Naval Postgraduate School, Monterey (Library)
3 Naval Ship Weapon Systems Engineering Station, Port Hueneme
    Code 5711, Repository (2)
    Code 5712 (1)

8 Naval Surface Weapons Center, Dahlgren
    G13
        D. Dickinson (1)
        T. Wasmund (1)
    G22, W. Holt (1)
    R15
        D. Houchins (1)
        M. Jamison (1)
        W. Smith (2)
    Technical Library (1)
8 Naval Surface Weapons Center, White Oak Laboratory, Silver Spring
    R10, S. Jacobs (1)
    R10B, M. Stosz (1)
    R12
        J. Erkman (1)
        L. Burke (1)
    R13, T. Liddiard (1)
    Guided Missile Warhead Section (1)
    Technical Library (1)
1 Naval War College, Newport
1 Naval Weapons Station, Concord (Code 321, M. Bucher)
1 Naval Weapons Station, Yorktown
    Code 50, L. Rothstein (1)
    Code 503, L. Leonard (2)
1 Office of Naval Research, Pasadena Branch Office
1 Office of Naval Technology, Arlington (ONT-07)
1 Operational Test and Evaluation Force, Atlantic
2 Pacific Missile Test Center, Point Mugu
    Code 1245, Nofrey (1)
    Technical Library (1)
1 Marine Corps Air Station, Beaufort
1 Army Armament Munitions & Chemical Command, Rock Island (DRSAR-LEP-L, Technical Library)
4 Army Armament Research and Development Command, Dover
    DRDAR-LCU-SS, J. Pentel (1)
    Technical Library (3)
1 Aberdeen Proving Ground (Development and Proof Services)
10 Army Ballistic Research Laboratory, Aberdeen Proving Ground
    AMSAA
        C. Alston (1)
        Blomquist (1)
    AMXAR-SEI-B (1)
    AMXAR-T, Detonation Branch (1)
    AMXAR-TSB-S (STINFO) (1)
    AMXBR-TBD
        J. Dahn (1)
        J. Kenecke (1)
    AMXBR-VLDA, T. Bentley (1)
    AMXSY-AD (1)
    AMXSY-J (1)
1 Army Materiel Systems Analysis Activity, Aberdeen Proving Ground (K. Meyers)
2 Army Research Office, Research Triangle Park
    DRXPO-IP-L, Information Processing Office (1)
    Dr. E. Saible (1)
1 Harry Diamond Laboratories, Adelphi (Technical Library)
1 Radford Army Ammunition Plant
1 Redstone Arsenal (Rocket Development Laboratory, Test and Evaluation Branch)
2 Rock Island Arsenal
    Navy Liaison Office (NVLNO) (1)
    Technical Library (SARRI-ADM-P) (1)
1 White Sands Missile Range (STEWS-AD-L)

END

2-87-

DTIC